

# Characterization of Autoemission Reflection for Precise Radiometer Calibration

A. J. Gasiewski,<sup>1</sup> D. Kraft,<sup>2</sup> and V. Leuski<sup>3</sup>

<sup>1</sup>Dept. of Electrical Computer and Energy Engineering,  
University of Colorado at Boulder  
0425 UCB, Boulder, CO 80309-0425, USA

[al.gasiewski@colorado.edu](mailto:al.gasiewski@colorado.edu)

<sup>2</sup>[david.kraft@colorado.edu](mailto:david.kraft@colorado.edu)

<sup>3</sup>[vladimir.leuski@colorado.edu](mailto:vladimir.leuski@colorado.edu)

## Abstract

Calibration of spaceborne microwave radiometers to precisions required for assessing climate trends requires biases less than 0.05 K to be identified. The use of warm pyramidal blackbody targets closely coupled to the radiometer antenna to establish thermal reference points has become standard for this purpose, although the effects of small standing waves generated by the radiometer itself can be considerable. We show these effects using a 55-GHz radiometer and precision scanned pyramidal target, along with coherent processing of the detected power. The study illustrates the importance of the radiometer front-end architecture in minimizing standing wave biases.

## 1. Background

The use of spaceborne microwave radiometers to measure subtle global brightness temperature trends that may be related to climate trends is predicated on the ability to calibrate to absolute accuracies commensurate with the anticipated level of climate-induced variation. To this end, it has been determined that the lower tropospheric temperature has been observed using Microwave Sounding Unit (MSU) data to be increasing at a rate of  $\sim 0.07^\circ\text{C}$  per decade [1]. In order to observe this signal unambiguously from satellites, and thus to be able to use the uniform global sensing capabilities offered by satellites to diagnose causes, the long-term absolute accuracy of satellite radiometers needs to be of order 50 mK or better. Such accuracy can potentially be achieved either vicariously [e.g., 2] or by regression of measurable thermal forcings to the calibration system after launch, although these methods are considered to be a secondary means by which to achieve a primary sensor requirement. A more desirable means of achieving such accuracy is to ensure, by design, that the emission temperatures of the calibration reference measurements on the instrument are repeatable to this level of precision, or better.

Many spaceborne microwave radiometers rely on the use of two external calibration references: cold space and a warm blackbody target. The former has a well-established temperature of  $2.725 \pm 0.002$  K [3] provided that lunar, solar, and/or terrestrial contamination of the field of view of the beam and (at frequencies near 1413 MHz) galactic emission caused by hydrogen are compensated. The latter have emission temperatures that drift with orbital phase due to diurnal and seasonal insolation changes. Changes in spacecraft and sensor thermal state caused by cycling of heaters, component efficiency changes due to aging, and surface reflectivity degradation can also impact the emission from the warm calibration target. While the physical temperature of an extended target can readily and repeatably be measured to within  $\sim 10$  mK using only a moderately sized array of thermistors, the reflection of energy from the target needs to be considered in calibration.

Of particular interest in this study is the reflection of microwave radiation produced by the radiometer itself (“autoemission”). For a typical close-coupled warm target this radiation reflects directly back into the radiometer feedhorn and contributes to the detected power. Ideally, reflected radiation causes a constant additive bias, but if the geometric distance between the target and feedhorn changes by even a small fraction (typically as small as  $\sim \lambda/16$ ) the standing wave produced by this radiation will affect the amplitude of the reflected noise at the receiver, and thus introduce a time-varying bias to the detected power. For bands that are essential to temperature and water vapor sounding of the atmosphere (50-57 and  $\sim 183$  GHz) the critical perturbation distances are as small as 0.3 and 0.1 mm, respectively. Future THz receivers for ice cloud measurements will result in even smaller critical distances. Given that it is difficult to control feedhorn-warm target geometry over the lifetime of a sensor to such levels it is

important to understand the degree to which variations in the autoemission standing wave ratio (SW) affect the detected power in radiometer systems.

## 2. Experimental Setup

Autoemitted signals are due to two primary sources: 1) Johnson thermal noise emitted by active or passive components in the radiometer RF front end, e.g., isolators, low noise amplifiers (LNAs), mixers, and couplers; and 2) local oscillator leakage out of the RF port of any mixer that may be present. The latter can be minimized by use of RF ferrite isolators or LNAs, or outright eliminated by direct detection. However, direct detection over numerous narrow-band radiometric channels remains hardware-intensive at millimeter-wave (MMW) and higher frequencies, and even LNAs and isolators provide only a limited degree of LO attenuation. Moreover, given that the LO frequency is usually placed slightly out-of-band of the forward transmission spectrum of the LNA or isolator, inadvertent out-of-band reverse LO transmission can be large, permitting significant leaked LO power to be radiated.

To study these effects a laboratory model of the 50-57 GHz sounding radiometer proposed for use on the NPOESS (now DWSS) Microwave Imager Sounder (MIS) sensor was implemented. The model used an RF front end virtually identical to that of the radiometer architecture being proposed for MIS, including feedhorn dimensions and incorporation of an isolator, LNA, and upper-sideband superheterodyne receiver. For simplicity, only a single-channel IF filter of 300 MHz bandwidth providing an RF response centered at 55 GHz was implemented. To examine the impact of the isolator and LNA in reducing autoemission SW effects both of these components were removable, requiring only a minor video gain adjustment.

The radiometer was mounted inside a thermally stable 1.8m x 1.5m x 1.2m MMW anechoic chamber with the feedhorn viewing the center of a pyramidal iron-epoxy calibration target. This target is also a prototype of that intended for use on the MIS. The pyramidal target was supported by a computer numerical controlled (CNC) milling machine interfaced to the radiometer computer, and thus was able to be step-positioned along three axes over a distance of ~30 cm with a repeatable precision of ~15  $\mu\text{m}$  (or,  $\sim\lambda/420$  at 55 GHz). Starting at a distance of 1.5 mm from the feedhorn aperture the target was repeatedly stepped in distance away from the feedhorn while the radiometer voltage was sampled. Typical sweep and sampling parameters are listed in Table 1.

**Table 1.** Sweep and sampling parameters for 55 GHz autoemission reflection measurements from a pyramidal target.

Parameter (55 GHz sweeps)	Value
Range of target axial motion	8.712 cm (3.430") or $16.00\lambda$
Minimum target-to-feedhorn aperture (gap) distance	0.15 cm (0.059") or $0.275\lambda$
Step increment	0.0170 cm (0.0067") or $0.0313\lambda$
Number of samples per sweep	512
Number of full scans	40 (80 one-way sweeps)
Elementary sample period	2.5 msec
Number of elementary samples averaged per (reported) sample	300
Effective integration time per sample	0.75 seconds
Total effective integration time per run	512 min
Total run time	1482 min (24.7 hours)
Integration efficiency	34.5%
Temperature stability in chamber (typical)	1-2 K

## 3. Coherent Data Processing

Data from successive swept measurements were calibrated into brightness temperature variations, then coherently averaged to remove the considerable amount of  $1/f$  drift inherent in total power radiometers sampled over periods longer than a few seconds (Figure 1). For these studies sampling occurred over durations exceeding 24 hours, resulting in drifts of up to ~50 K. The autoemission SW standard deviation  $\sigma_{\text{SW}}$  was calculated from the coherently averaged brightness data. If  $\sigma_{\text{Di}}$  is the standard deviation of the raw calibrated data over the  $i^{\text{th}}$  sweep and  $\sigma_{\langle\text{D}\rangle}$  is the standard deviation taken over the average of a set of  $2N$  sweeps of data (i.e., 2 sweeps for each full back and forth scan), then the following relationships hold:

$$\begin{aligned}
\langle \sigma_{D_i}^2 \rangle &= \sigma_{SW}^2 + \Delta T_{RMS}^2 + \sigma_{1/f}^2 \\
\sigma_{\langle D \rangle}^2 &= \sigma_{SW}^2 + \frac{\Delta T_{RMS}^2 + \sigma_{1/f}^2}{2N_{sweeps}} \\
\therefore \sigma_{\langle D \rangle}^2 &= \sigma_{SW}^2 + \frac{\langle \sigma_{D_i}^2 \rangle - \sigma_{SW}^2}{2N_{sweeps}} \\
\Rightarrow \sigma_{SW}^2 &= \left( \sigma_{\langle D \rangle}^2 - \frac{\langle \sigma_{D_i}^2 \rangle}{2N_{sweeps}} \right) \left( 1 - \frac{1}{2N_{sweeps}} \right)^{-1}
\end{aligned}$$

where  $\Delta T_{RMS}$  and  $\sigma_{1/f}$  are the standard deviations of the integration and  $1/f$  noise, respectively. These noise contributions are assumed to be independent from sweep to sweep. Using 40 full sweeps the SW STD  $\sigma_{SW}$  was readily computable to a precision of ~10-20 mK.

Fourier analysis of the coherently averaged data permit unambiguous identification of the source of the autoemission (Figure 2). Spectral peaks observed at twice the measured spatial frequency in (cycles/mm) correspond to the wavelength of either the local oscillator when autoemission is dominated by LO leakage or of the RF passband when autoemission is dominated by Johnson thermal noise originating from the isolator/LNA/mixer. Figure 2 shows the spectrum of a scan observing a flat aluminum reflector to exaggerate this effect, for clarity.

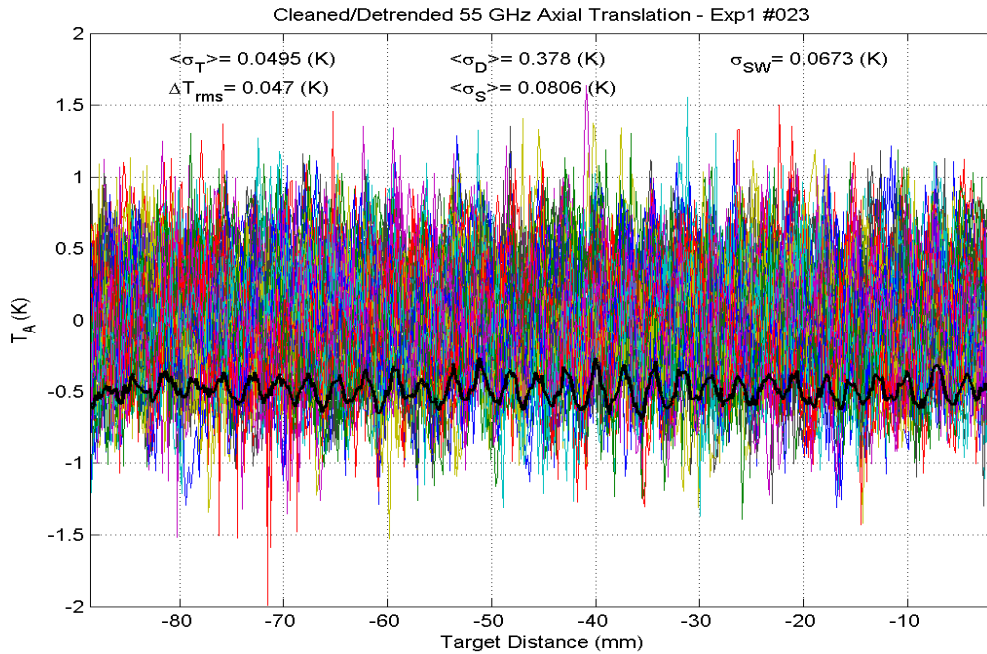


**Figure 1.** Example of raw Tb data from 80 brightness temperatures sweeps observing a pyramidal iron-epoxy target, along with coherently averaged signal showing autoemission standing wave behavior. An LNA with no isolator was used for this experiment.

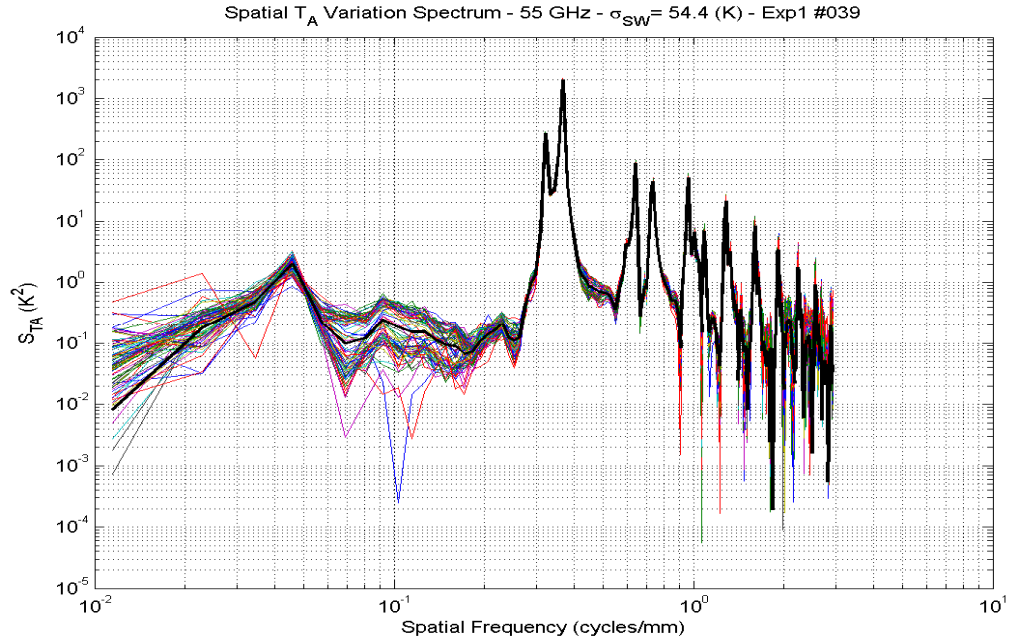


**Figure 2.** Fourier spectra of brightness scans for an experiment using no LNA nor isolator and observing a flat aluminum reflector. In this case the impact of autoemission reflection from both LO and thermal sources is clearly seen in the two strong peaks at 0.31 and 0.35 cycles/mm (respectively).

#### 4. Impact of Radiometer Architecture on Autoemission STD $\sigma_{SW}$

The use of both an isolator and LNA significantly reduced the reflected autoemission SW signal standard deviation from a pyramidal iron epoxy target and USB superheterodyne radiometer at 55 GHz to acceptable levels of  $\sim 20$  mK. Such absolute calibration uncertainties are suitable for long-term climate studies. However, removal of (first) the isolator, and then (successively) the LNA, raised the autoemission SW standard deviation to 0.05-0.07 and 0.15-0.25K, respectively. These values were seen to be dependent on the geometrical parameters (specifically, the pyramid height), and hence the actual reflectivity of the targets. Improved target design would serve to reduce autoemission standard deviation, and would be particularly important at higher frequencies where isolators are currently unavailable and LNAs are relatively expensive.

#### 5. References

- [1] Wentz, F., and M. Schabel, "Effects of Orbital Decay on Satellite-Derived Lower-Tropospheric Temperature Trends," *Nature*, 394, 661-664, 13 August 1998.
- [2] Ruf, C.S. "Detection of Calibration Drifts in Spaceborne Microwave Radiometers Using a Vicarious Cold Reference," *IEEE Trans. Geosci. Remote Sens.*, 38(1), 44-52, 2000.
- [3] Mather, J. C., Fixsen, D. J., Shafer, R. A., Mosier, C., and Wilkinson, D.T. "Calibrator Design for the COBE Far-Infrared Absolute Spectrophotometer (FIRAS)," *Astrophysical Journal*, vol. 512, issue 2, pp. 511-520, 1999.